Electronic Supplementary Information for

Ultrasensitive and Highly Selective Detection of Formaldehyde via an Adenine-Based Biological Metal-Organic Framework

Yu-Bai Wei,[a,+] Ming-Jie Wang,[c,+] Dong Luo,[a] Yong-Liang Huang,[d] Mo Xie,[a] Weigang Lu,*[,a,b] Xugang Shu*[,c] and Dan Li*[,a,b]

[a] College of Chemistry and Materials Science, Jinan University, Guangzhou 510632, P. R. China

[b] Guangdong Provincial Key Laboratory of Functional Supramolecular Coordination Materials and Applications, Jinan University, Guangzhou 510632, P. R. China

[c] Department College of Chemistry and Chemical Engineering, Zhongkai University of Agriculture and Engineering, Guangzhou 510225, P. R. China

[d] Department of Chemistry, Shantou University Medical College,Shantou, Guangdong 515041, P. R. China

[+] Y.-B. W. and M.-J. W. contributed equally

Table of Contents

Experimental Section

Synthesis of $H_2BPDC\text{-}(NH_2)_2$

The $H_2BPDC\text{-}(NH_2)_2$ was synthesized according to previous reports with modifications.[1,2,3,4]

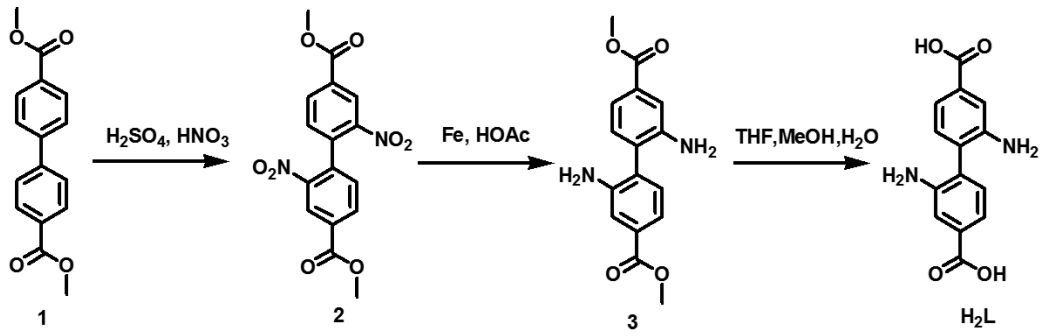

Scheme S1. Synthetic route for **$H_2BPDC\text{-}(NH_2)_2$** (H_2L).

Dimethyl-2,2′-dinitro-[1,1′-biphenyl]-4,4′-dicarboxylate 2:

Dimethyl-biphenyl-4,4′-dicarboxylate **1** (5.00 g, 18.5 mmol) was added into concentrated H_2SO_4 (50 mL). The mixture was stirred at room temperature for 10 min. Then, a premixed nitric acid (56%, 15 mL) and concentrated sulfuric acid (15 mL) was added dropwise at room temperature over a period of 20 min. The resulting mixture was stirred vigorously for 2 h at below room temperature and then carefully poured onto crushed ice (300 g). The pale yellow precipitated was filtered, washed with water until neutral pH, air-dried, and vacuum-dried (100 °C) to produce **1** (1.2 g, 90%). ^{1}H-NMR (400 MHz, DMSO-d_6): δ 8.69 (s, 2H, H_{Ph}), 8.38 (d, J = 8.0 Hz, 2H, H_{Ph}), 7.71 (d, J = 8.0 Hz, 2H, H_{Ph}), 3.96 (s, 6H, H_{Me}).

Dimethyl-2,2′-diamino-[1,1′-biphenyl]-4,4′-dicarboxylate 3:

Dimethyl-2,2′-dinitro-[1,1′-iphenyl]-4,4′-dicarboxylate **2** (1.0 g, 2.8 mmol) was dissolved in 30 mL of acetic acid and then iron powder (4.75 g, 85 mmol) was added. The mixture was stirred for 20 h at room temperature under argon atmosphere. The suspension was filtered through Celite and evaporated. The residue was dissolved in ethyl acetate and H_2O. The organic layer was washed by conc. $NaHCO_3$ (aq.) and brine, dried over $MgSO_4$, and filtered. The solvent was removed by rotary evaporation, yielding **3** as a yellow powder (0.89 g, 89 %). ^{1}H-NMR (400 MHz, DMSO-d_6): δ 7.44 (s, 2H, H_{Ph}), 7.23 (d, J = 7.8 Hz, 2H, H_{Ph}), 7.08 (d, J = 7.8

Hz, 2H, H_{Ph}), 5.00 (s, 4H, H_{NH2}), 3.84 (s, 6H, H_{Me}).

2,2´-Diamino-[1,1´-biphenyl]-4,4´-dicarboxylic acid (H_2BPDC-$(NH_2)_2$):

Dimethyl 2,2´-diamino-[1,1´-biphenyl]-4,4´-dicarboxylate **3** (2.0 g, 6.7 mmol) was dissolved in 40 mL of THF/MeOH (v/v, 1:1) and then 20 mL of aqueous NaOH (0.6 M) was added dropwise under vigorous stirring. The mixture was stirred overnight at room temperature. The organic solvent was removed under vacuum at 40 °C and the aqueous solution was acidified with excessive amount of HCl to yield a light brown solid, which washed with abundant cold water and air-dried to afford the desired product (735 mg, 2.7 mmol, 90%). ^{1}H-NMR (400 MHz, DMSO-d_6): δ 12.87 (s, 2H, H_{COOH}), 7.62 (s, 2H, H_{Ph}), 7.45 (d, J = 7.8 Hz, 2H, H_{Ph}), 7.23 (d, J = 7.9 Hz, 2H, H_{Ph}).

Synthesis of Crystals and Complexes

Synthesis of JNU-100

A mixture of Zn(NO3)2·6H2O (160.8 mg, 0.54 mmol), adenine (12.2 mg, 0.09 mmol), 2,2'-Diamino-[1,1'-biphenyl]-4,4'-dicarboxylic acid (35.4 mg, 0.13 mmol), DMF/H2O (12 mL, 10:1, v/v), and nitric acid (68%, 0.07 mL) was introduced into a 25 mL of Parr Teflon-lined stainless steel vessel and heated at 135 °C for 3 days. Then it was cooled naturally to room temperature. The formed crystals (JNU-100) were filtered, washed with DMF, and air-dried (Yield: 72.94 mg, 35 %). IR (KBr pellet, cm–1): 3334 (m), 1655 (w), 1605(s), 1548 (s),1740 (w), 1368 (s), 1214(m), 1152 (m), 839 (w), 777 (m), Elemental analysis (CHN), C86H106N40O21Zn6, calculated (%): C 42.47, H 4.39, N18.43; found (%): C 42.57, H 4.11, N 18.08.

Synthesis of HCHO@JNU-100

As-synthesized **JNU-100** was soaked in 37% HCHO for 3 days, then washed with CH3OH and air-dried to afford **HCHO@JNU-100**. IR (KBr pellet cm–1): 3222 (w), 3133 (m), 1597 (s), 1564 (s), 1417(w), 1339 (s), 1226 (m), 1095 (s), 1006 (w), 939 (w), 904 (w), 844 (w), 784(s), 675 (w), 501 (w). Elemental analysis (CHN), C109H198N30O80Zn6, calculated (%): C 36.48, H 5.56.77, N11.71; found (%): C 36.54, H 4.202, N 11.69.

Synthesis of JNU-100@PCL

The **JNU-100@PCL** test strips were prepared according to the literature[5] with some modifications. In a typical procedure, 20 mg of MOF material was dispersed in dichloromethane (DCM, 500 μL) to give a suspension A; 200 mg of polycaprolactone (PCL, MW: 80000) was dissolved in DCM (1.50 mL) to give a solution B. Suspension A was sonicated for 30 min and then mixed with solution B. After stirring for another 30 min, it was carefully cast onto a flat glass substrate, followed by slow vaporization of solvent by placing it on a hot plate maintained at 37 °C. About 3 h later, **JNU-100@PCL** test strips were peeled off the glass substrate and dried under vacuum at room temperature.

Synthesis of JXNU-4

The **JXNU-4** was synthesized according to the literature.[6]

Synthesis of HCHO@JXNU-4

As-synthesized **JXNU-4** was soaked in 37% HCHO for 3 days, washed with CH3OH, and air-dried to afford **HCHO@JNU-4**.

Fluorescence Interference Experiments

An aqueous solution was prepared containing the following VOCs (each 0.2 M): HCHO, TEA, methanol, THF, isopropyl alcohol, acetone, DMSO, ethanediol, EtOH, 1,4-Dioxane, acetic acid, 1-butanol, DMF, and DMA. 0.3 mL of the above mixed VOCs solution was added to 2.7 mL of aqueous suspension of **JNU-100** (0.2 mg/mL) and its fluorescence emission was measured after shaking.

^{1}H-NMR Spectrum of Ligand

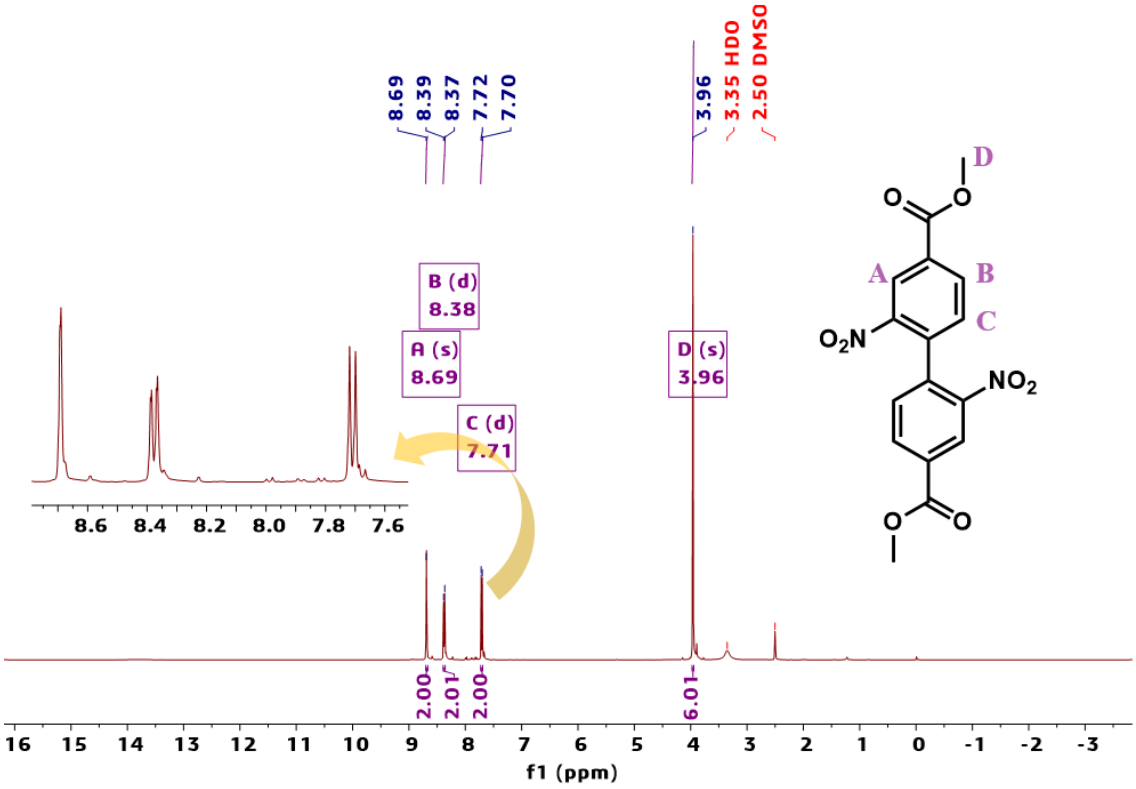

Figure S1. ^{1}H-NMR spectrum of dimethyl-2,2´-dinitro-[1,1´-biphenyl]-4,4´-dicarboxylate **2**.

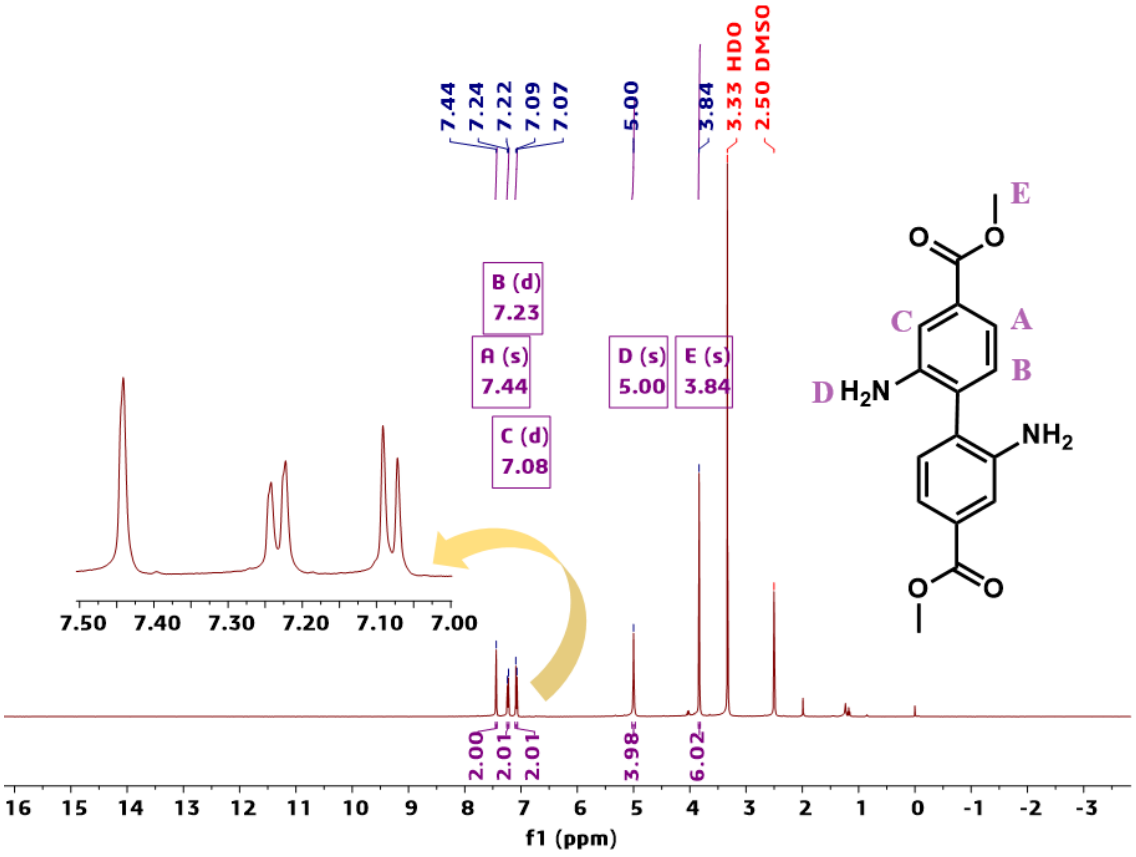

Figure S2. ^{1}H-NMR spectrum of dimethyl-2,2´-diamino-[1,1´-biphenyl]-4,4´-dicarboxylate **3**.

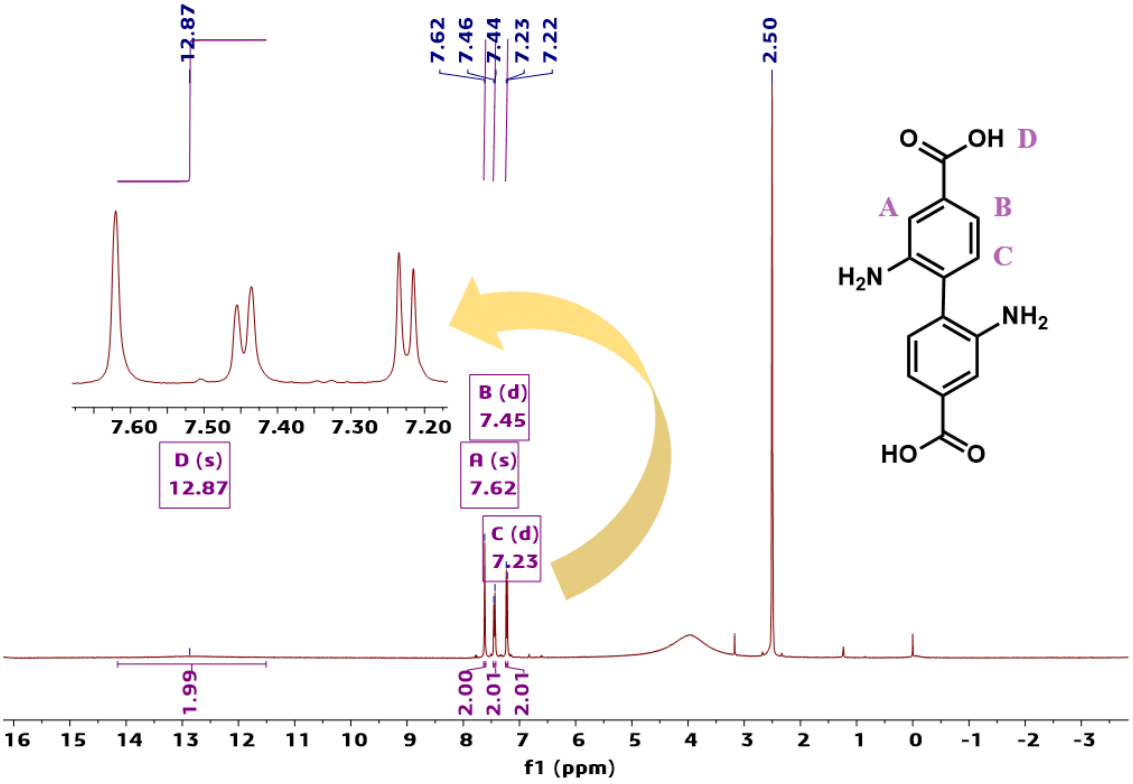

Figure S3. ^{1}H-NMR spectrum of 2,2´-diamino-[1,1´-biphenyl]-4,4´-dicarboxylic acid (**H_2bpdc-(NH_2)$_2$**).

Structure Section

Single-Crystal X-ray Crystallography

Single-crystal X-ray diffraction data collections were implemented on an Oxford Cryo stream system on a XtaLAB PRO MM007-DW diffractometer (Rigaku, Cu Kα, λ = 1.54184 Å) equipped with a graphite monochromator and Pilatus3R-200K-A detector at 100 or 293 K. The Structures were solved using direct methods and refined with full-matrix least-squares refinements using the SHELX2018/3 programs. All non-hydrogen atoms were refined by anisotropic thermal parameters, and the hydrogen atoms were formed geometrically. Some of the guest molecules in **JNU-100** and **HCHO@ JNU-100** were highly disordered and could not be located and refined successfully. SQUEEZE program of PLATON software was used to eliminate the scattering of guest molecules. Parameters for crystal data and refinements are summarized in **Table S1**. CCDC Nos. 1996163 for **JNU-100 (1)**, 1996162 for **HCHO@JNU-100 (2)**, and 2031977 for **HCHO@JXNU-4 (3)**.

Table S1. Crystal data and structure refinements for **1, 2,** and **3**

Compounds	**1**	**2**	**3**
Empirical formula	$C_{82}H_{70}N_{30}O_{19}Zn_6$	$C_{80}H_{63}N_{28}O_{21}Zn_6$	$C_{80}H_{56}N_{20}O_{21}Zn_6$
Formula weight	2171.90	2144.80	2025.66
Temperature/K	293(2)	100.01(13)	99.98(18)
Crystal system	tetragonal	tetragonal	orthorhombic
Space group	*P*4/*nnc*	*P*4/*nnc*	*Pnnn*
a/Å	26.1307(2)	25.8586(3)	20.9694(2)
b/Å	26.1307(2)	25.8586(3)	25.5976(2)
c/Å	20.4822(2)	21.0509(5)	26.1337(2)
α/°	90	90	90
β/°	90	90	90
γ/°	90	90	90
Volume/Å^3	13985.5(3)	14076.0(5)	14027.7(2)
Z	4	4	4
ρ_{calc}g/cm^3	1.032	1.012	0.959
μ/mm^{-1}	1.605	1.597	1.563
F(000)	4416.0	4348.0	4096.0
Radiation	Cu Kα (λ = 1.54184)	Cu Kα (λ =1.54184)	Cu Kα (λ = 1.54184)
2θ range/°	8.634 to 156.75	8.72 to 153.632	4.832 to 147.078
Reflections collected	41980	36634	50560
Independent reflections	7349 [R_{int} = 0.0279, R_{sigma} = 0.0182]	7156 [R_{int} = 0.0403, R_{sigma} = 0.0322]	13667 [R_{int} = 0.0390, R_{sigma} = 0.0360]
Data/restraints/parameters	7349/51/336	7156/450/465	13667/99/714
Goodness-of-fit on F^2	1.103	1.018	1.071
Final R indexes [I>=2σ (I)]	R_1 = 0.0586	R_1 = 0.0763	R1 =0.0618
	wR_2 = 0.1988	wR_2 = 0.2204	*w*R2 =0.1875

Final R indexes [all data]	R_1 = 0.0639	R_1 = 0.0931	R1 =0.0712
	wR_2 = 0.2048	wR_2 = 0.2500	wR2 =0.1988

^{a} $R_1 = \Sigma(||F_0|- |F_c||)/\Sigma|F_0|$; ^{b} $wR_2 = [\Sigma w(F_0^2- F_c^2)^2/\Sigma w(F_0^2)^2]^{1/2}$

Computational details

The initial structures for calculations were cut from the crystal structures including four Zn cations and the hydrogen atoms were used to saturated broken bonds. Density functional theory (DFT) and time-dependent density functional theory (TD-DFT) were performed here to obtain the vertical excitation energy and corresponding electronic transition based on the ground states. Theoretical level of B3LYP functional[7] and basis sets of LanL2DZ[8] for Zn and 6-31G (d)[9] for other atoms were used. The lowest-lying absorption with oscillator strength larger than 0.01 were selected analyze the nature of excited states. As for **HCHO@JNU-100(b)**, the strongest absorption at 367.7 nm is selected. All calculations were performed within Gaussian09 program.[10]

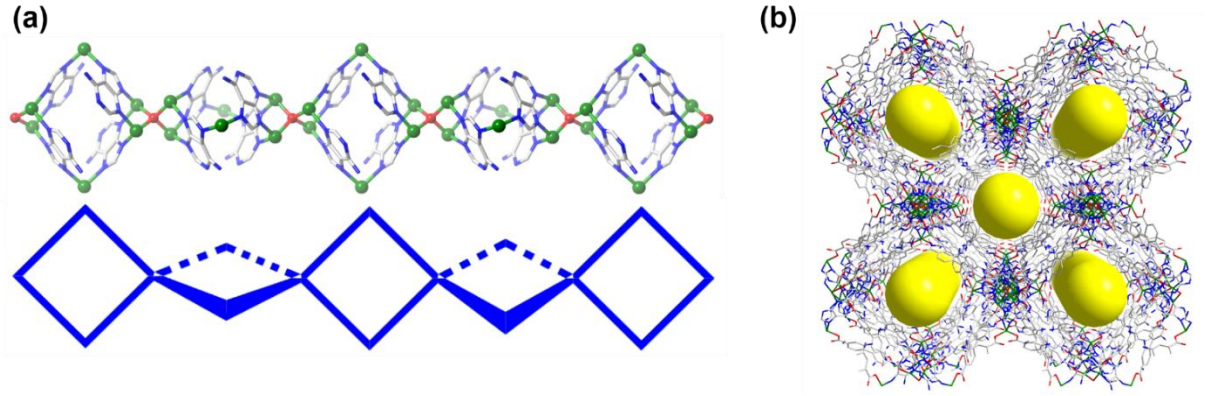

Figure S4. (a) A rod-like $[Zn_6(ad)_4(\mu_4\text{-O})]_n$ SBU highlighting an orthogonal arrangement of $[Zn_6(ad)_4]$ cages through μ_4-O. (b) Perspective view of the 3D crystal structure of **JNU-100** along the c axis (yellow cylinders represent 1D channels).

Structural Analysis

The suitable single crystals of **JNU-100**, **HCHO@JNU-100**, and **HCHO@JXNU-4** were selected and characterized with X-ray diffraction. **JNU-100** crystallizes in tetragonal space group *P4/nnc* (**Table S1**). One and half Zn^{II} ions, one μ_4-O^{2-} (O_5) with an occupation of 0.25; one ad^- and one L^{2-} are in the asymmetric unit (**Figure S4a**). The two crystalographically

independent Zn^{II} ions both display tetrahedral coordination geometry. Zn2 located at the 2-fold axis is coordinated by two imidazolate N atoms of two ad^- ligands and two carboxylate O atoms from two L^{2-} ligands to form a mononuclear tetracoordinated configuration. The distance between Zn2 and imidazole N on ad^- is 2.0397 (21) Å, whereas the distance between Zn2 and the carboxylate O of L^{2-} ligands is 1.9487 (17) Å. Meanwhile Zn1 atom is bonded to one imidazolate N atom and one pyrimidine N atom from two ad^- ligands and two O atoms from a L^{2-} ligand and a μ_4-O^{2-} to generate a Zinc oxygen tetrahedral structure. The distance between Zn1 and imidazole N and pyrimidine N on ad^- is 2.009 (21) Å and 2.0420 (23) Å, respectively; while the distance from Zn1 to carboxylate O on μ_4-O^{2-} and L^{2-} is 1.9795 (5) Å and 1.9833(20) Å, respectively. The ad^- ligand binds three Zn ions through its one pyrimidine N atom and two imidazolate N atoms. Two carboxylate O atoms of L^{2-} ligands are linked to two Zn ions; four μ_3-ad^- ligands bridge four Zn1 atoms and two Zn2 atoms to generate a $Zn_6(ad)_4$ cage, which dimensions is about 7.7473(38) × 10.1633(1) × 10.2411(1) $Å^3$. The adjacent $Zn_6(ad)_4$ cages are linked by μ_4-O^{2-} through the Zn-O bonds to give a 1D infinite columnar $[Zn_6(ad)_4(\mu_4\text{-}O)]_n$ SBU featuring O-centered tetrahedral $[Zn_4(\mu_4\text{-}O)]$ units. Within the 1D columnar $[Zn_6(ad)_4(\mu_4\text{-}O)]_n$ SBU, each $Zn_6(ad)_4$ cage is surrounded by eight L^{2-} with two monodentate carboxylate groups. The $(BPDC\text{-}2NH_2)^{2-}$ ligands link the 1D columnar $[Zn_6(ad)_4(\mu4\text{-}O)]$ nSBUs to form an anionic 3D framework. The 3D framework with double walls possesses 1D square channels running along the c axis with dimensions of 11.12(44) × 11.12(31) $Å^2$, wherein the DMF and H_2O molecules are housed. The resultant 3D framework of the **JNU-100** overall charge is balanced by dimethylammonium cations ($Me_2NH_2^+$) generated *in situ* from the decomposition of DMF solvent molecules.

HCHO@JNU-100 is isomorphic to **JNU-100** except that the amino groups on adenines formed hemiaminal with formaldehyde. The whole framework has not changed significantly.

Topological Analysis

For comprehending the underlying topology, a rigorous topological identification for the net of **JNU-100** was computed by the program Systre and TOPOS. From a topological point of view, both BPDC-$(NH_2)_2$ and adenine can be simplified as di-topic linkers and the two clusters as 4- and 8-connected nodes, respectively (**Fig. S5**). Thus, the structure of **JNU-100** can be simplified

as a (4, 8)-c network with the point symbol of $\{4^{10}.6^{16}.8^2\}$ $\{4^5.6\}_2$ and transitivity of [2253].

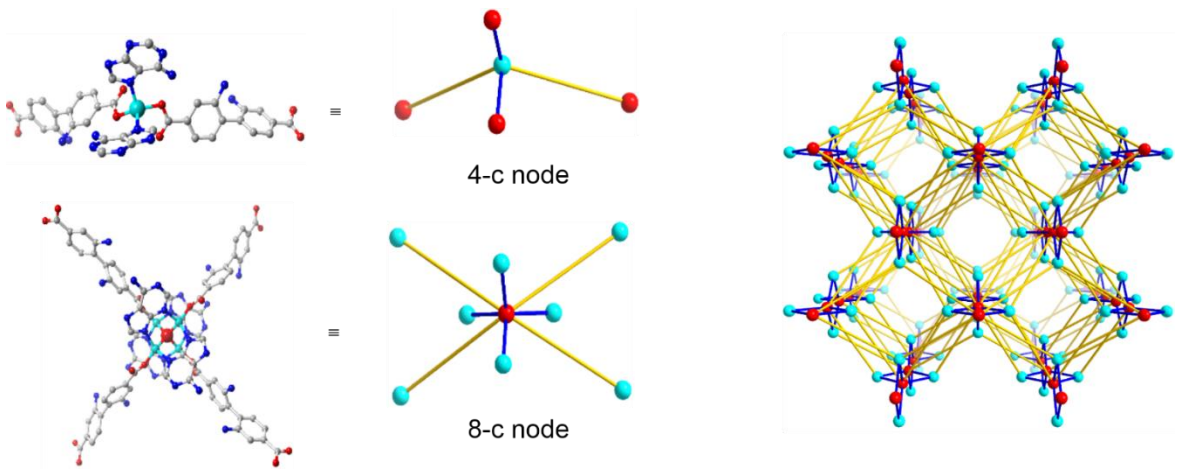

Figure S5. Underlying topology of **JNU-100** with the point symbol of $\{4^{10}.6^{16}.8^2\}$ $\{4^5.6\}_2$; red ball, 8-connected node (Zn_4O cluster); cyan ball, 4-connected node (mononuclear Zn cluster); yellow stick, di-topic linker (BPDC-$(NH_2)_2$ and adenine).

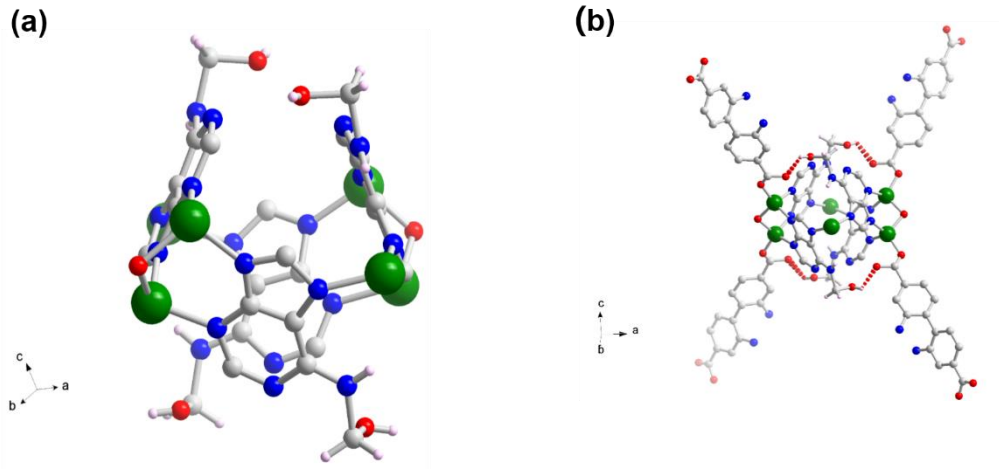

Figure S6. (a) The crystal structure of **HCHO@JNU-100** showing the formed hemiaminals. (b) View of the intermolecular interactions in **HCHO@ JNU-100**. Color codes: Zn, sea green; C, grey; N, blue; O, red.

Characterization Section

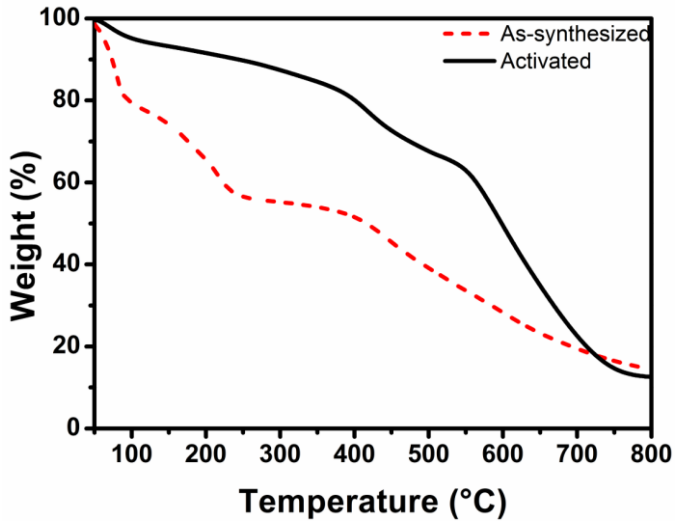

Figure S7. TGA of **JNU-100**, dashed line represented as-synthesized; solid line represented activated**.**

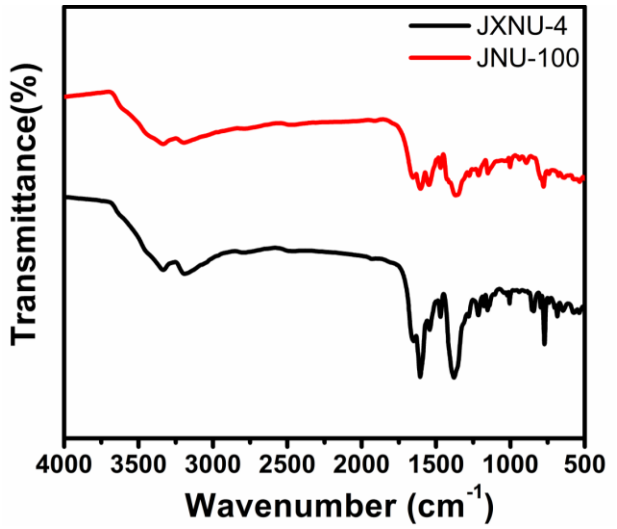

Figure S8. IR spectra of **JNU-100** and **JXNU-4.**

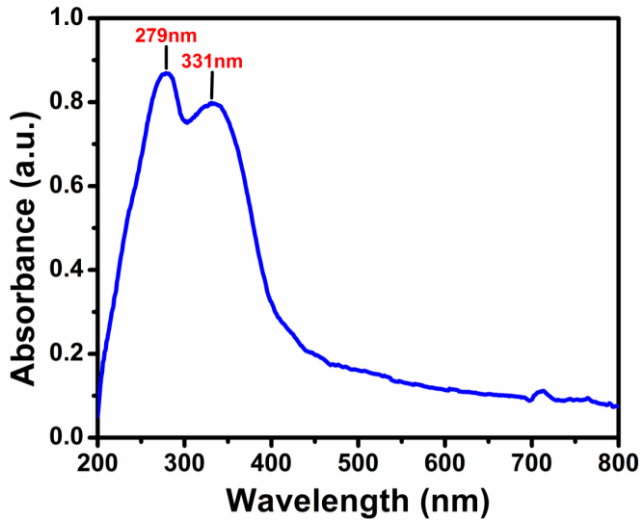

Figure S9. Solid-state UV absorption spectra of **JNU-100.**

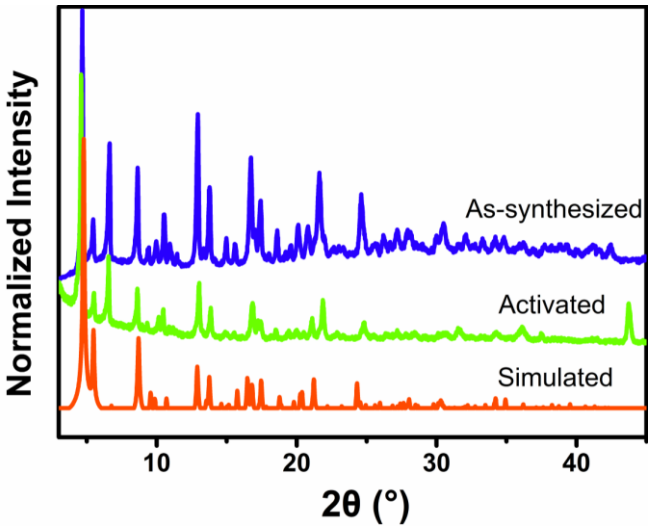

Figure S10. PXRD patterns of **JNU-100**.

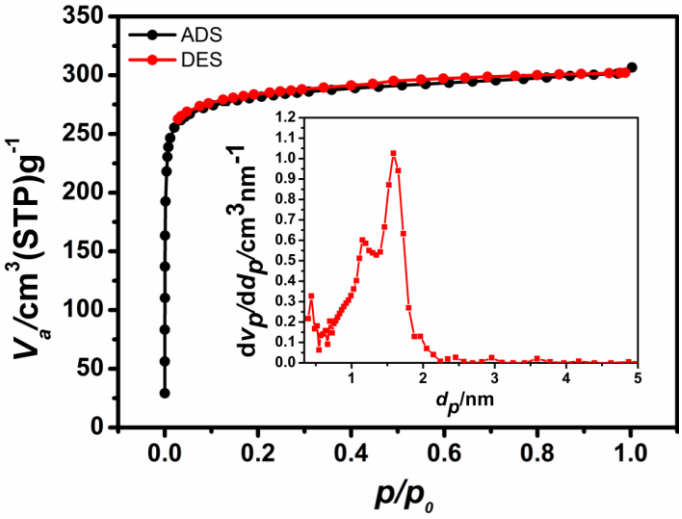

Figure S11. N_2 adsorption and desorption isotherm at 77K for **JNU-100**, and the inset is pore size distribution plot.

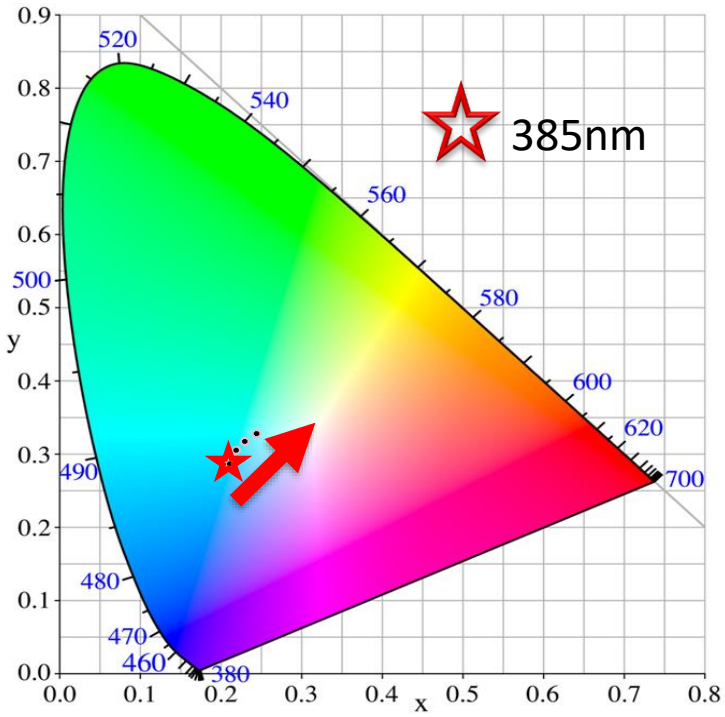

Figure S12. CIE-1931 chromaticity diagram. The black dots signify the emission color coordinates for the different excitation wavelengths.

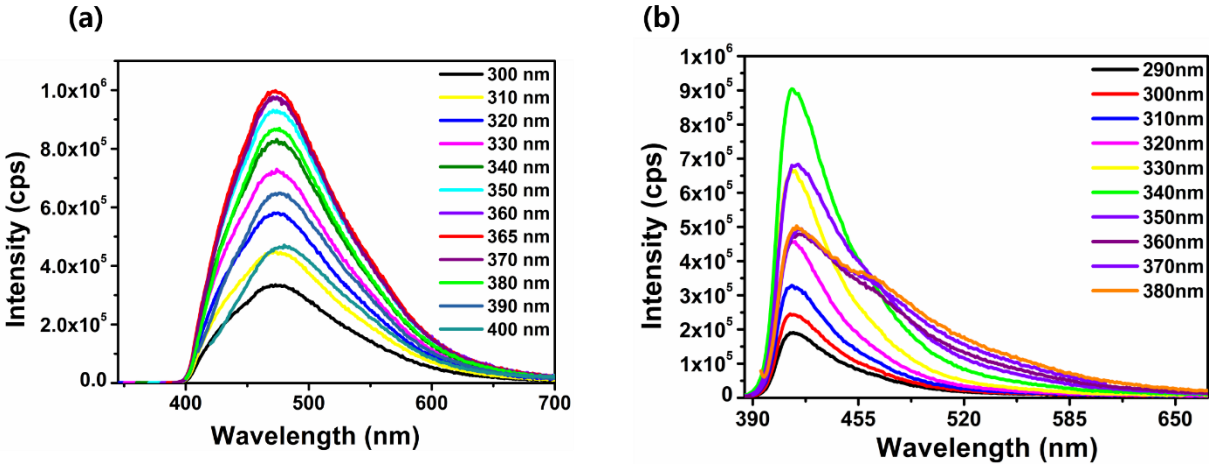

Figure S13. Excitation-energy-varied emission spectra of **JNU-100** (a) and **JXNU-4** (b).

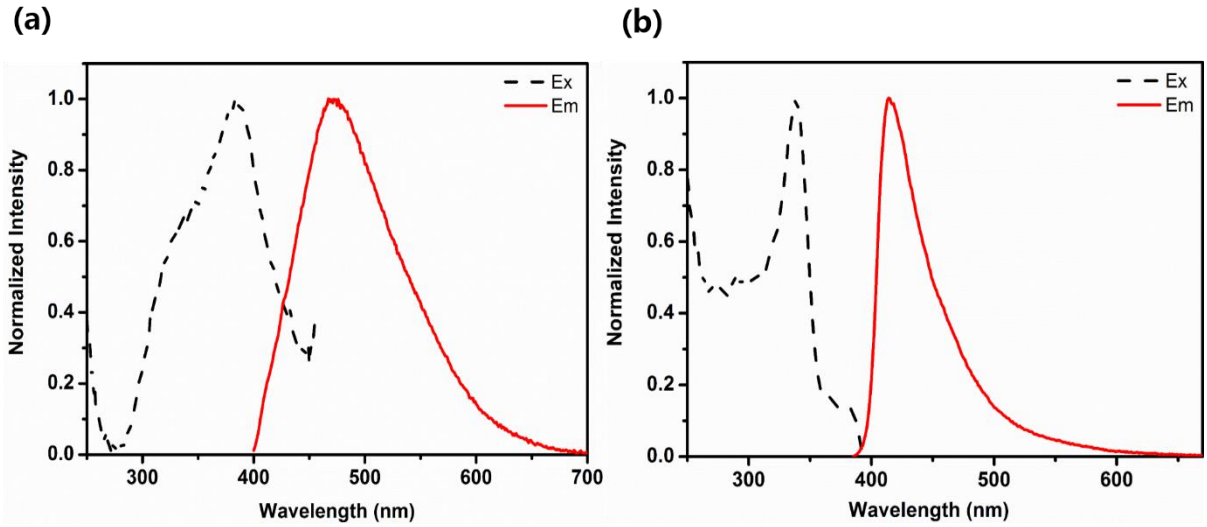

Figure S14. Excitation and emission spectra of **JNU-100** with optimal excitation wavelength at 385 nm and emission wavelength at 485 nm (a) and **JXNU-4** with optimal excitation wavelength at 328 nm and emission wavelength at 414 nm (b).

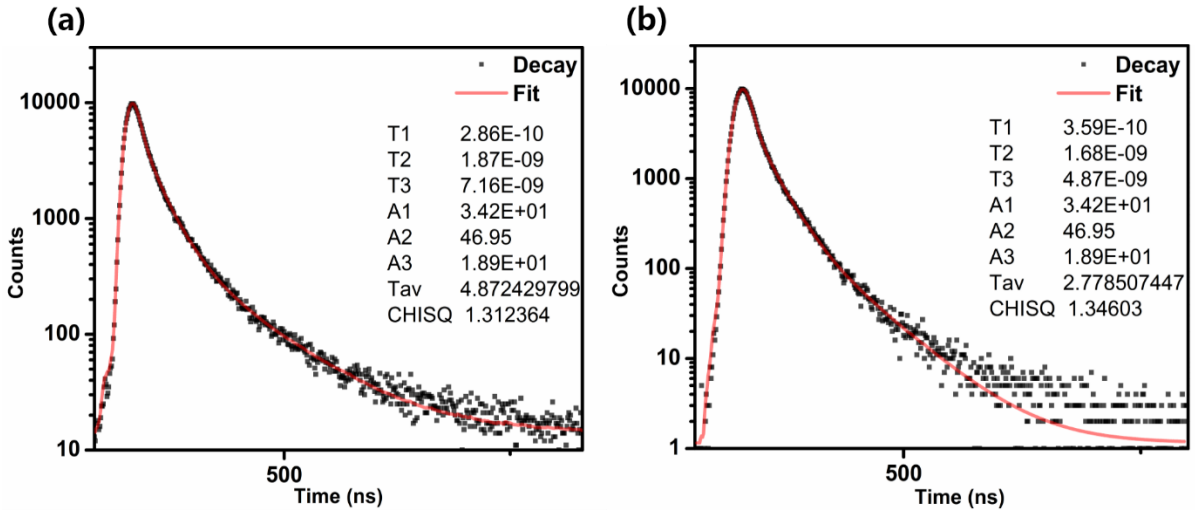

Figure S15. Fluorescence lifetime measurements for powder samples of **JNU-100** (a) and **JXNU-4** (b) at room temperature under ambient environment.

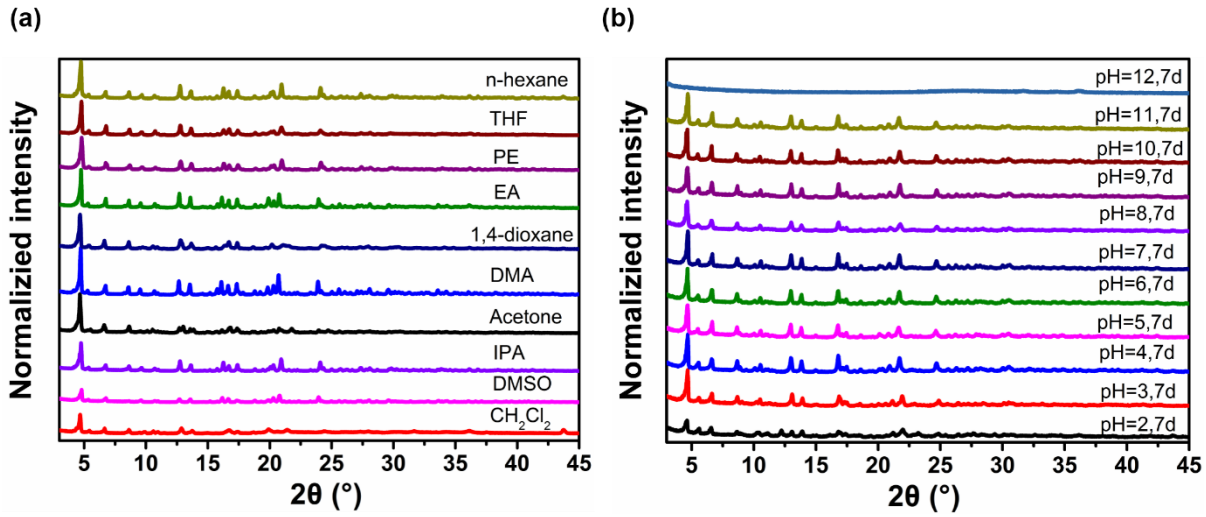

Figure S16. PXRD patterns of **JNU-100** after soaking in organic solvents (left) and in acidic and alkali solutions for 7 days (right).

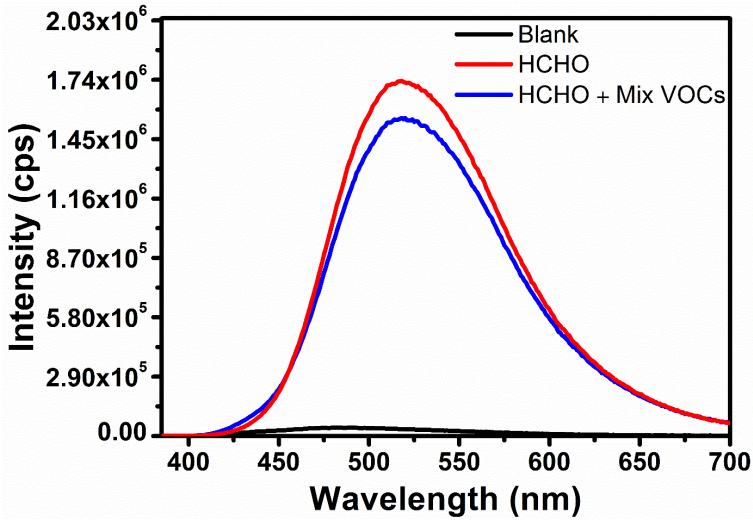

Figure S17. Fluorescence spectra of an aqueous suspension of **JNU-100** (black), upon addition of HCHO (0.10 M) (red), and upon addition of HCHO (0.10 M) and a mixture of VOCs (14.29 mM each) (blue).

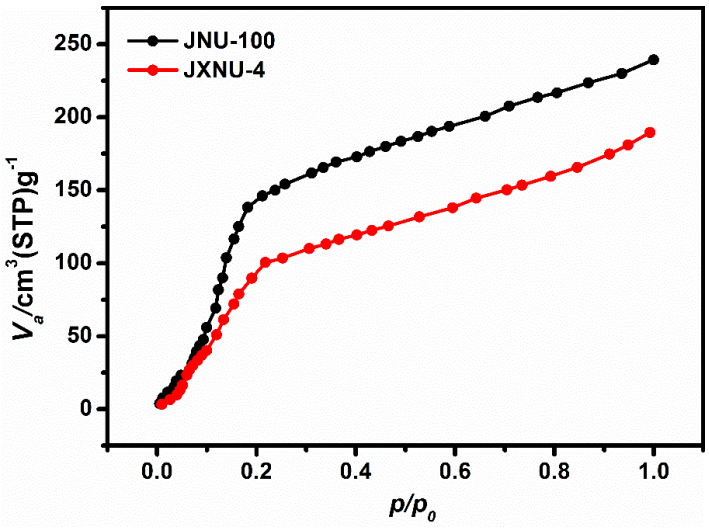

Figure S18. Water vapor adsorption isotherms of **JNU-100** and **JXNU-4** at 298k.

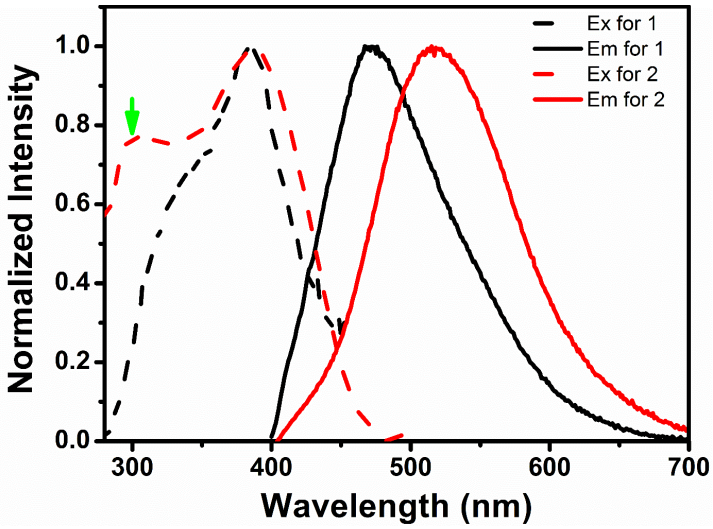

Figure S19. Comparison of the excitation (dashed) and emission (solid) spectra of **JNU-100** in aqueous solution (1) and in 0.10 M HCHO solution (2).

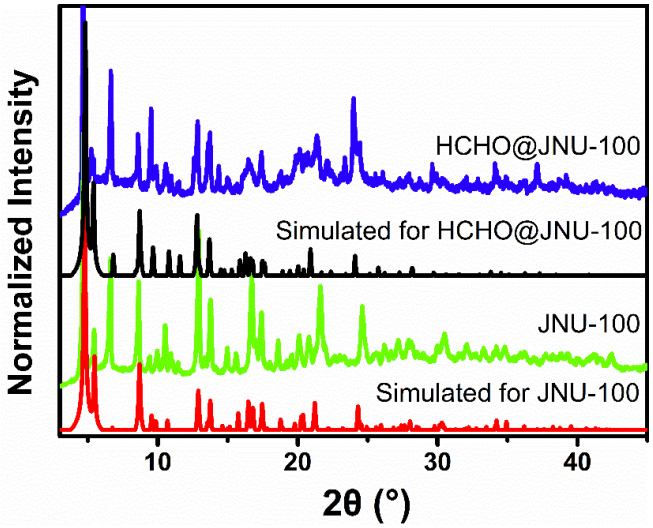

Figure S20. Comparison of PXRD patterns of **JNU-100** and **HCHO@JNU-100**.

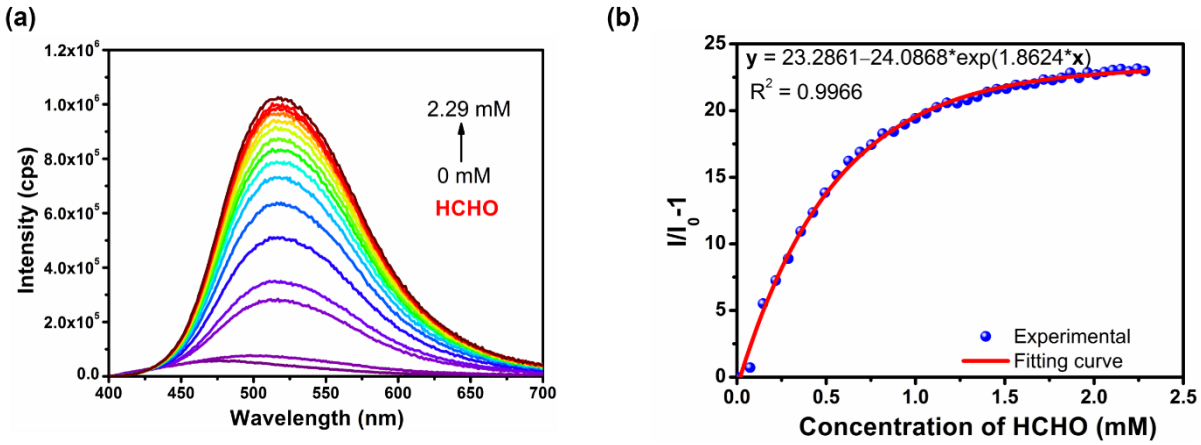

Figure S21. (a) Fluorescence emission spectra of aqueous suspensions of **JNU-100** (0.2 mg/mL) excited at 365 nm upon the incremental addition of HCHO (10 mM). (b) The corresponding exponent relationship between I/I_0-1 and the HCHO concentration based on the concentration-dependent fluorescence titration experiments.

Table S2. The simulated lowest-lying absorptions and the corresponding electronic transitions.

	wavelength / nm	*f*	Transition	Assignment
JNU-100	310.4	0.030	H-1-L+7 (36.2%) H-3-L+7 (32.5%) H-1-L+8 (14%)	LC&LLCT
HCHO@JNU-100(a)	336.9	0.064	H-L+5 (66.1%) H-1-L+4 (23.2%)	LC&LLCT
HCHO@JNU-100(b)	367.7	0.003	H-7-L+2 (90.9%)	LLCT&MLCT

(a) and (b) refer to the two sets of disordered structure of **HCHO@JNU-100**, *f* refers to oscillator strength

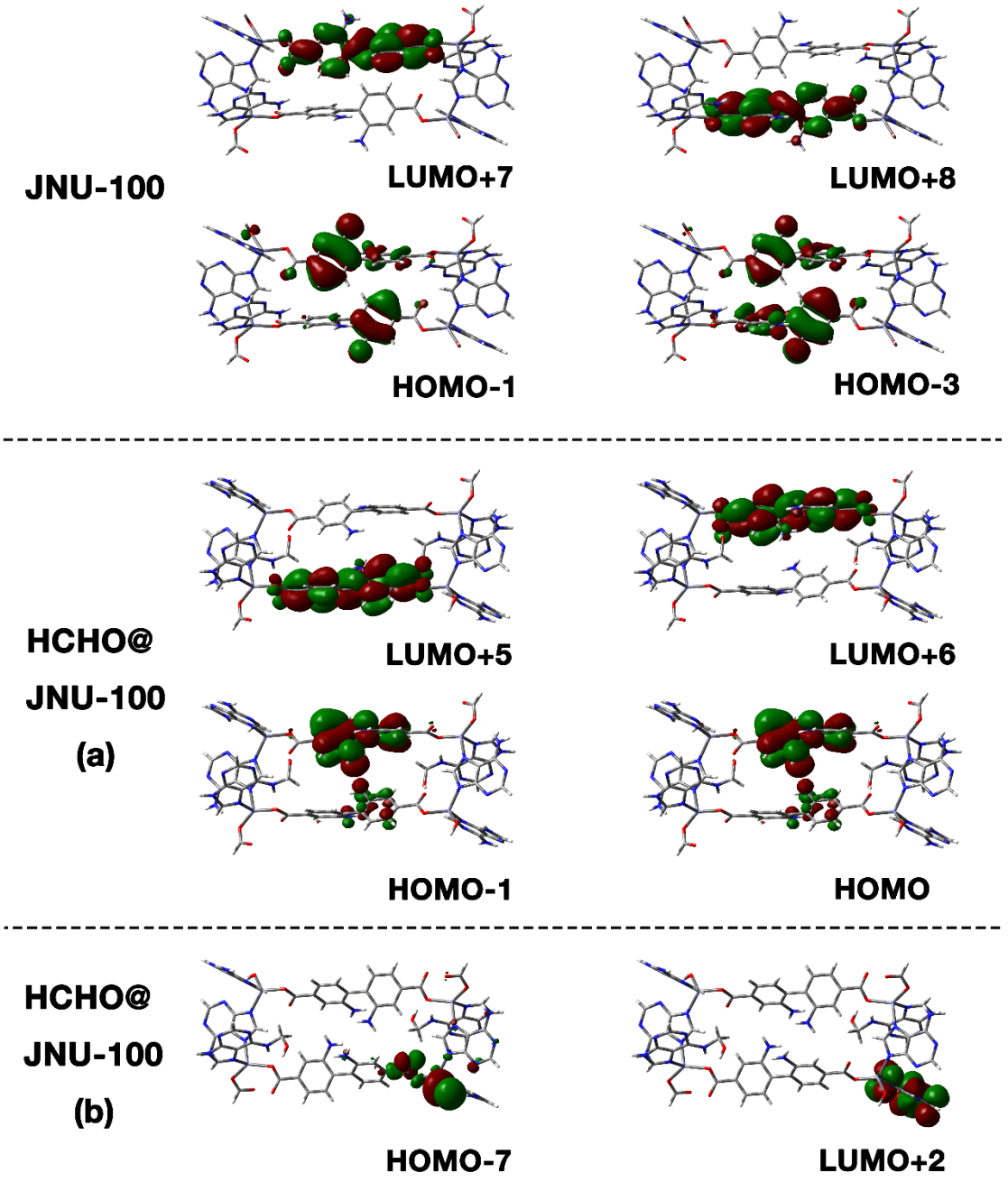

Figure S22. Representative molecular orbital diagrams of **JNU-100** and **HCHO@JNU-100**.

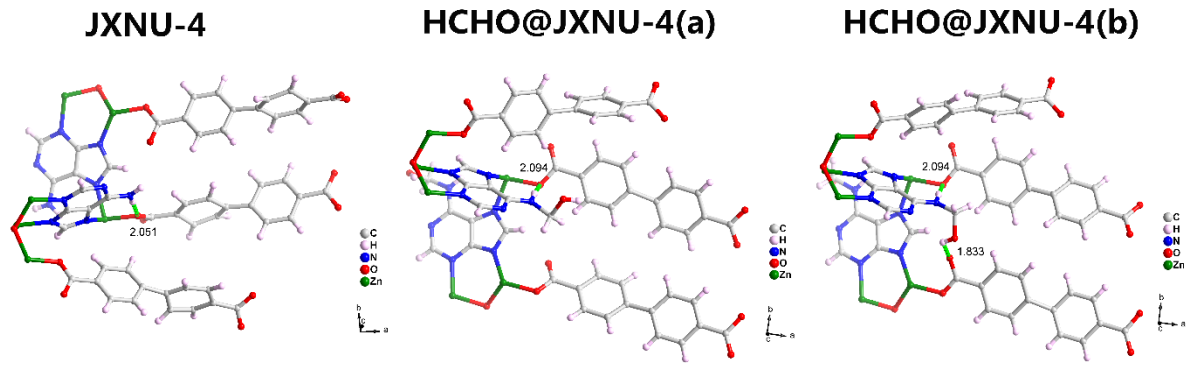

Figure S23. The crystal structure of **HCHO@JXNU-4** (the distance unit in the figure is Å)

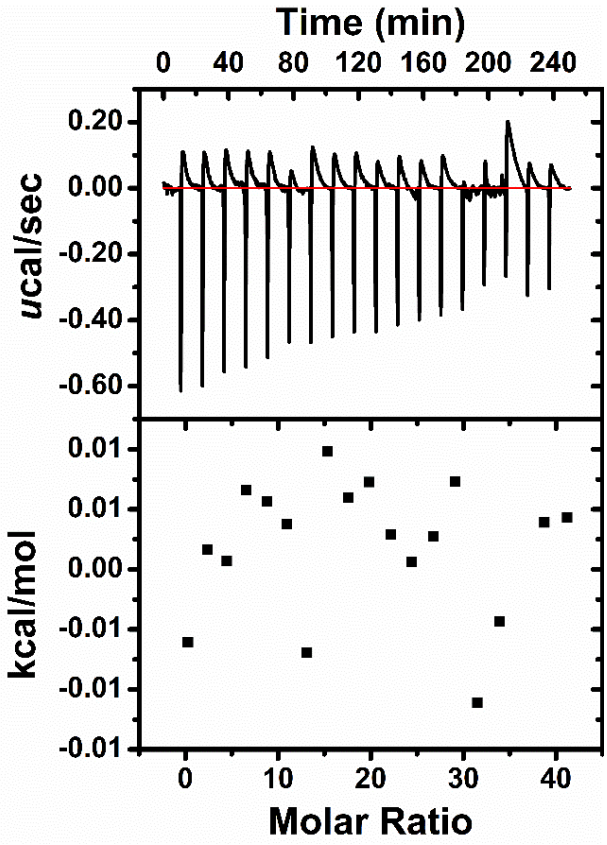

Figure S24. ITC thermogram resulting from the titration of a **JXNU-4** suspension (0.50 mM, 1.8 mL) with a HCHO solution (100 mM, 300 μL, 15 μL each injection).

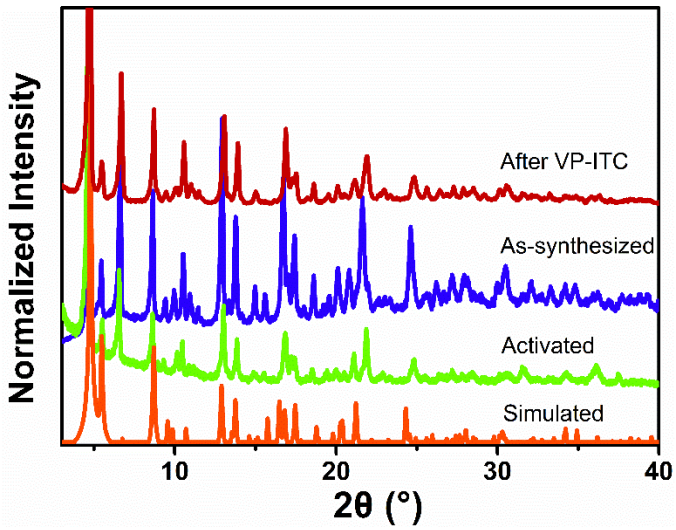

Figure S25. PXRD patterns of **JNU-100** after VP-ITC experiments.

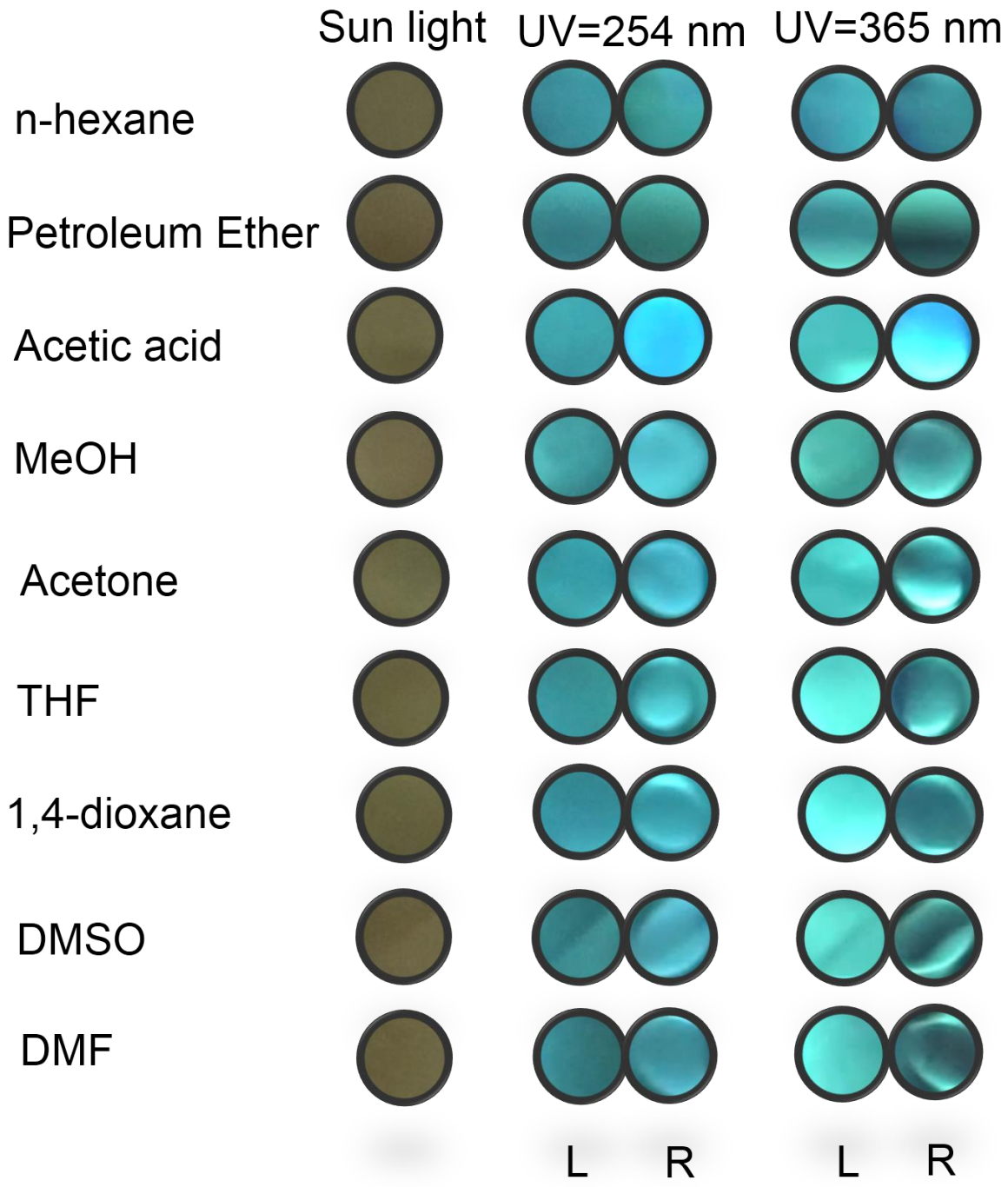

Figure S26. Photographs of **JNU-100@PCL** without HCHO (L) and with 0.10 M HCHO (R) under UV light.

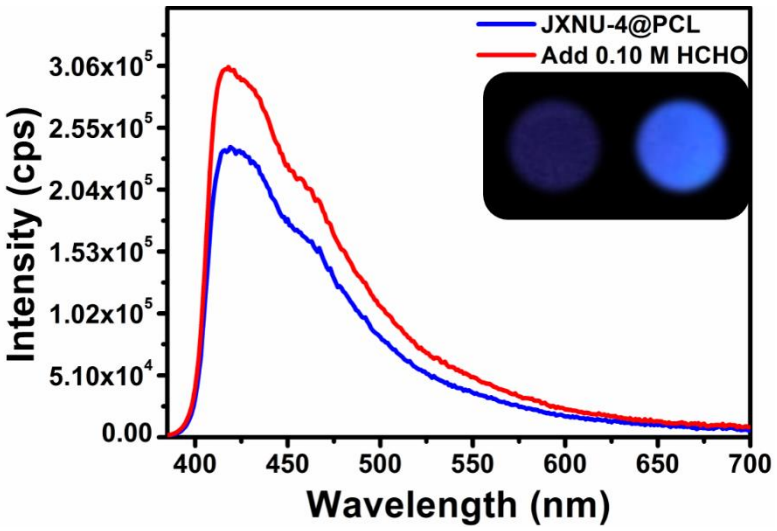

Figure S27. Emission spectra of **JXNU-4@PCL** upon addition of 0.10 M HCHO under UV light (excited at 365 nm), the inset photographs denote the sample without (L) and with 0.10 M HCHO (R), respectively.

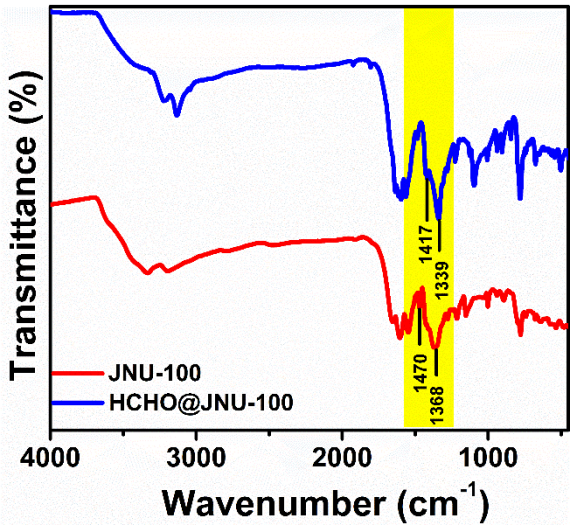

Figure S28. IR spectra of **JNU-100**; **HCHO@JNU-100** highlighting the wavenumber changes upon hemiaminal formation.

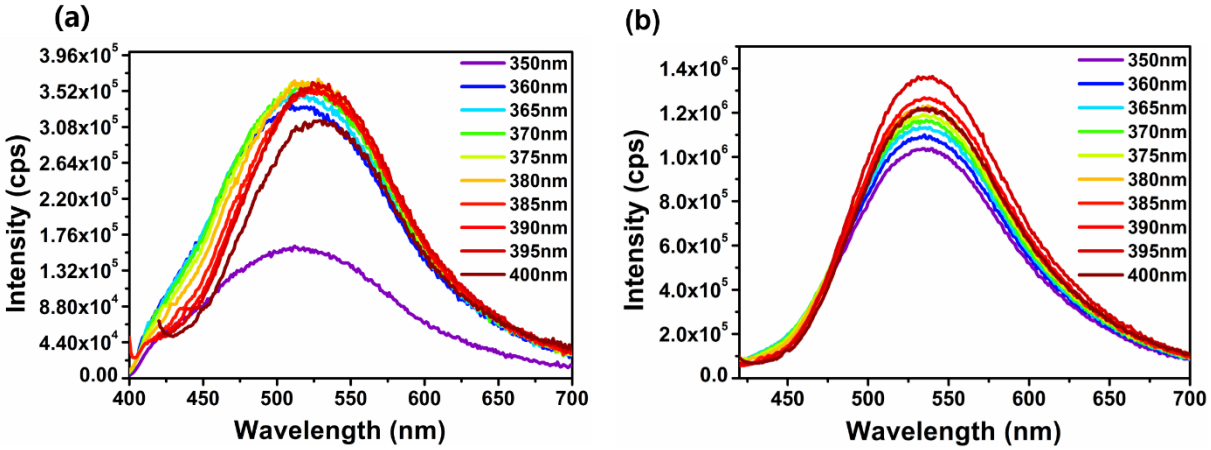

Figure S29. Excitation-energy-varied emission spectra of **JNU-100@PCL** without HCHO (a) and with 0.10 M HCHO (b).

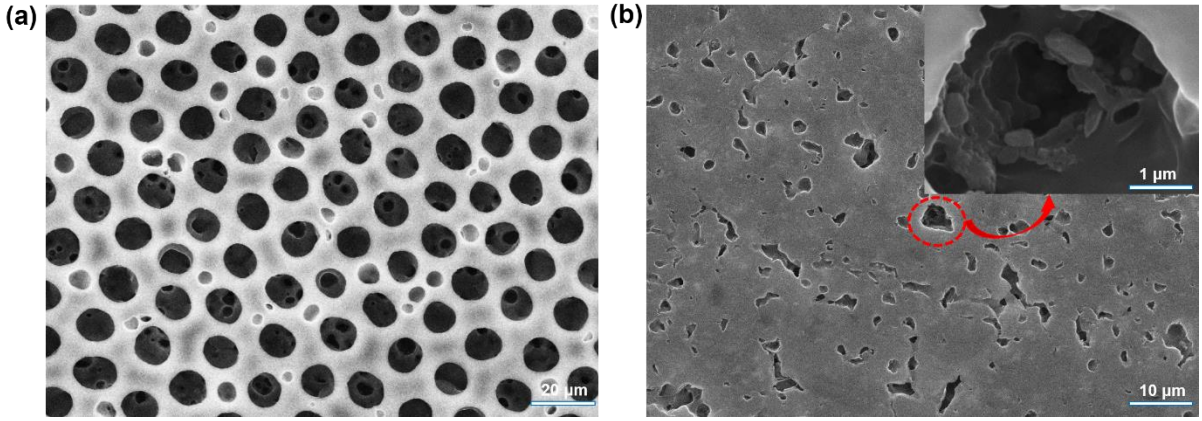

Figure S30.SEM images of PCL (a) and **JNU-100@PCL** (b).

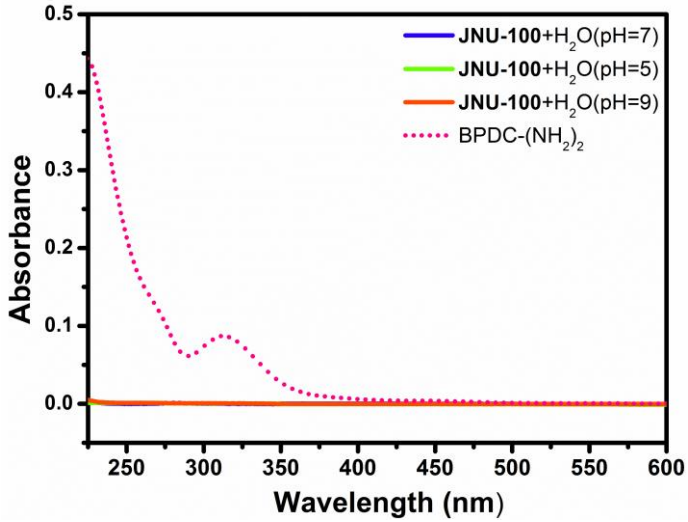

Figure S31. UV-vis absorption spectra of the supernatants of **JNU-100** aqueous suspensions at different pHs, indicating no ligand leaching under either acidic or basic conditions.

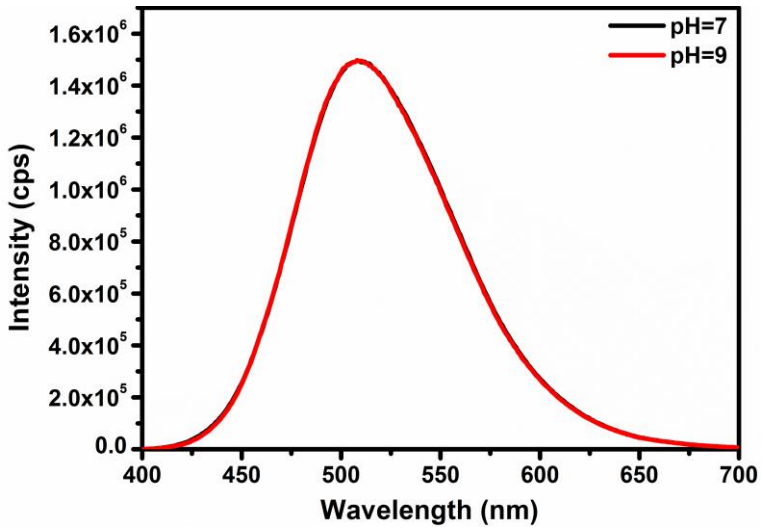

Figure S32. Fluorescence spectra of **JNU-100** aqueous suspensions upon addition of HCHO (0.10 M) at pH = 7 (black) and pH = 9 (red).

Notes and References

(1) Gil-San-Millan, R.; Lopez-Maya, E.; Hall, M.; Padial, N. M.; Peterson, G. W.; DeCoste, J. B.; Rodriguez-Albelo, L. M.; Oltra, J. E.; Barea, E.; Navarro, J. A. R. Chemical Warfare Agents Detoxification Properties of Zirconium Metal-Organic Frameworks by Synergistic Incorporation of Nucleophilic and Basic Sites. *ACS Appl Mater Interfaces* **2017**, *9*, 23967-23973.

(2) McDonald, K. A.; Ko, N.; Noh, K.; Bennion, J. C.; Kim, J.; Matzger, A. J. Thermal decomposition pathways of nitro-functionalized metal-organic frameworks. *Chem. Commun.* **2017**, *53*, 7808-7811.

(3) Qin, T.; Gong, J.; Ma, J.; Wang, X.; Wang, Y.; Xu, Y.; Shen, X.; Zhu, D. A 3D MOF showing unprecedented solvent-induced single-crystal-to-single-crystal transformation and excellent CO_2 adsorption selectivity at room temperature. *Chem. Commun.* **2014**, *50*, 15886-15889.

(4) Ko, N.; Hong, J.; Sung, S.; Cordova, K. E.; Park, H. J.; Yang, J. K.; Kim, J. A significant enhancement of water vapour uptake at low pressure by amine-functionalization of UiO-67. *Dalton Trans.* **2015**, *44*, 2047-2051.

(5) Liu, M.; Wang, L.; Zheng, X.; Xie, Z. Zirconium-Based Nanoscale Metal–Organic Framework/Poly(ε-caprolactone) Mixed-Matrix Membranes as Effective Antimicrobials. *ACS Appl. Mater. Interfaces* **2017**, *9*, 41512-41520.

(6) Ma, H. F.; Liu, Q. Y.; Wang, Y. L.; Yin, S. G. A Water-Stable Anionic Metal-Organic Framework Constructed from Columnar Zinc-Adeninate Units for Highly Selective Light Hydrocarbon Separation and Efficient Separation of Organic Dyes. *Inorg. Chem.* **2017**, *56*, 2919-2925.

(7) Becke, A. D. Density‐functional thermochemistry. III. The role of exact exchange. *J. Chem. Phy.* **1993**, *98*, 5648-5652.

(8) Check, C. E.; Faust, T. O.; Bailey, J. M.; Wright, B. J.; Gilbert, T. M.; Sunderlin, L. S. Addition of polarization and diffuse functions to the LANL2DZ basis set for P-Block elements. *J. Phys. Chem. A* **2001**, *105*, 8111-8116.

(9) Hehre, W. J.; Ditchfield, R.; Pople, J. A. Self—consistent molecular orbital methods. XII. Further extensions of Gaussian—type basis sets for use in molecular orbital studies of organic molecules. *J. Chem. Phy.* **1972**, *56*, 2257-2261.

(10) M. J. Frisch, G. W. T., H. B. Schlegel, G. E. Scuseria, M. A. Robb, J. R. Cheeseman, G. Scalmani, V. Barone, B. Mennucci, G. A. Petersson, H. Nakatsuji, M. Caricato, X. Li, H. P. Hratchian, A. F. Izmaylov, J. Bloino, G. Zheng, J. L. Sonnenberg, M. Hada, M. Ehara, K. Toyota, R. Fukuda, J. Hasegawa, M. Ishida, T. Nakajima, Y.

Honda, O. Kitao, H. Nakai, T. Vreven, J. A. Montgomery, Jr., J. E. Peralta, F. Ogliaro, M. Bearpark, J. J. Heyd, E. Brothers, K. N. Kudin, V. N. Staroverov, R. Kobayashi, J. Normand, K. Raghavachari, A. Rendell, J. C. Burant, S. S. Iyengar, J. Tomasi, M. Cossi, N. Rega, J. M. Millam, M. Klene, J. E. Knox, J. B. Cross, V. Bakken, C. Adamo, J. Jaramillo, R. Gomperts, R. E. Stratmann, O. Yazyev, A. J. Austin, R. Cammi, C. Pomelli, J. W. Ochterski, R. L. Martin, K. Morokuma, V. G. Zakrzewski, G. A. Voth, P. Salvador, J. J. Dannenberg, S. Dapprich, A. D. Daniels, Ö. Farkas, J. B. Foresman, J. V. Ortiz, J. Cioslowski, and D. J. Fox, Gaussian, Inc., Wallingford CT, Gaussian 09, Revision D.01,. *Gaussian, Inc.Wallingford CT,* **2009**,